Rigid-unit modes in tetrahedral crystals

2007 J. Phys.: Condens. Matter 19 406218

(http://iopscience.iop.org/0953-8984/19/40/406218)

IOP PUBLISHING JOURNAL OF PHYSICS: CONDENSED MATTER

J. Phys.: Condens. Matter **19** (2007) 406218 (17pp) doi:10.1088/0953-8984/19/40/406218

Rigid-unit modes in tetrahedral crystals

Franz Wegner

Institut für Theoretische Physik, Universität Heidelberg, Philosophenweg 19, D-69120 Heidelberg, Germany

Received 29 March 2007, in final form 22 August 2007
Published 12 September 2007
Online at stacks.iop.org/JPhysCM/19/406218

Abstract

The 'rigid-unit mode' (RUM) model requires unit blocks, in our case tetrahedra of SiO_4 groups, to be rigid within first order of the displacements of the oxygen ions. The wavevectors of the lattice vibrations, which obey this rigidity, are determined analytically. Lattices with inversion symmetry yield generically surfaces of RUMs in reciprocal space, whereas lattices without this symmetry yield generically lines of RUMs. Only in exceptional cases such as in β-quartz does a surface of RUMs appear, if inversion symmetry is lacking. The occurrence of planes and bending surfaces, and straight and bent lines, is discussed. Explicit calculations are performed for five polymorphs of SiO_2 crystals.

1. Introduction

Displacements of ions in a solid, which alter the distances between neighbouring ions, produce much stronger forces than those which vary only the angles between adjacent bonds. This has led to the idea of rigid-unit modes (RUMs), that is, distortions, which do not change the distances between the ions in a unit to first order in the displacements. Typical examples are crystals in which silicon or aluminium ions are surrounded by four oxygen ions. The units of the tetrahedra of these oxygens are required to be rigid. Each oxygen ion belongs to two tetrahedra.

There have been extensive numerical studies of RUMs of such crystals by Dove, Giddy, Hammonds and Heine *et al*. For a review see [1]. More recent presentations of RUMs in framework aluminosilicates can be found on the internet [2] and in the review [3]. These rigid-unit modes do not only signal soft-phonon modes, but they are also at the origin of a large number of displacive phase transitions. The first one considered was the transformation between α- and β-quartz [4]. Recent applications of RUM modelling include basic ideas for the development of new zeolites [5]. These zeolites are important catalysts in petrochemical refineries due to their high internal surface areas and molecular sieving properties. Another application deals with the flexibility of framework structures, which due to RUMs allows cation substitutions with a minimum of energy cost, since the geometric stress associated with the substitution is absorbed by rigid-unit-type motion of the polyhedra near the substitution site [6].

0953-8984/07/406218+17$30.00

Basic to the numerical calculations is the computer program CRUSH [7, 8]. In this program the rigid tetrahedra are assumed to be individual molecules, and harmonic forces are added between the two 'split' atoms, which should be one. It calculates the phonon frequencies $\omega_{j,\mathbf{q}}$ for given wavevector $\mathbf{q}$, which allow one to determine a pseudo-intensity

$$I(\mathbf{q}) = \sum_j \frac{1}{\omega_{j,\mathbf{q}}^2 + \Omega} \tag{1}$$

evaluated for small Ω. For a wavevector $\mathbf{q}$ with n RUMs this quantity approaches $I(\mathbf{q}) \approx n/\Omega$. In this way the authors determined RUMs for a large number of crystals.

There are also some analytic calculations along planes and lines of symmetry. Such a calculation has been performed by Vallade *et al* [9] for β-quartz. The concept of RUMs itself goes back to Megaw [10] and Grimm and Dorner [4].

The present paper reports analytic calculations of RUMs. The variation of the lengths of the bonds of the units is calculated as a function of the displacements of the O ions. Since the number of coordinates of the displacements is the same as the number of lengths of bonds, namely six times the number of tetrahedra, one has to find non-trivial solutions of linear homogeneous equations, which means the determination of the zeros of the determinant of the corresponding coefficient matrix. In reciprocal space these reduce to $6n_\mathrm{t}$ equations, where n_t is the number of tetrahedra in the unit cell of the crystal. So one has to calculate the determinant of a $6n_\mathrm{t} \times 6n_\mathrm{t}$ matrix, where the vector $\mathbf{q}$ of the oscillating wave of displacements and the basis vectors $\mathbf{a}_k$ of the lattice enter only through the three complex phase factors

$$\rho_k = \mathrm{e}^{\mathrm{i}\mathbf{a}_k\cdot\mathbf{q}}. \tag{2}$$

We will show that for a crystal with inversion symmetry the determinant of an appropriately defined matrix is real for any given ρs. Thus there is only one condition to be met with three unknowns, which in general defines the surfaces of the RUMs in reciprocal space. If inversion symmetry is lacking, then the determinant is complex, and two conditions have to be met for the RUMs: both the real and the imaginary part have to vanish. Correspondingly, RUMs are found only at the intersections of the zeros of the real and the imaginary part. Thus generically one obtains in these cases lines of RUMs, but not surfaces. It may happen, however, that both the real and the imaginary part have a factor in common, so that RUMs extend over a whole surface. An example is β-quartz, where a whole plane of RUMs, besides lines of RUMs, is found. Although in many cases the RUMs are located on planes or lines, there are also cases where a surface can bend, as was already found for HP (hexagonal primitive) tridymite by Dove *et al* [11]. Here (equation (53)) the analytic expression for the surface is given. Lines of RUMs may lie in planes. But there are also non-planar lines. Such a line has been found in α-quartz (figure 6).

The general theory is given in section 2. Some remarks on planes and bending surfaces, and straight and bent lines are given in section 2.1. The basic equations will be derived in section 2.2. In particular the coefficient matrix for the determinant will be given. In section 2.3 the consequences of inversion symmetry will be considered. It will be shown that the determinant multiplied by appropriate powers of ρ_k is real for lattices with inversion symmetry. This section is concluded with a few remarks on the actual algebraic calculation in section 2.4.

This theory is applied to five polymorphs of SiO_2 in section 3: first the crystals with inversion symmetry β-cristobalite and HP tridymite are considered, then the RUMs for the crystals without inversion symmetry β-quartz, α-cristobalite, and α-quartz are calculated.

2. General idea

2.1. Planes and bending surfaces, and straight and bent lines

The determinant (or its real and imaginary part) is factorized after calculation. The factorization procedure of algebraic computer programs is very useful, since the zeros of the various factors yield different locations of the RUMs. Often factors of the form

$$\rho_1^{l_1}\rho_2^{l_2}\rho_3^{l_3} \mp \rho_1^{l_1'}\rho_2^{l_2'}\rho_3^{l_3'} \tag{3}$$

with integer powers l_i and l_i' appear. Then the determinant (or its real or imaginary part) vanishes along the plane

$$[(l_1 - l_1')\mathbf{a}_1 + (l_2 - l_2')\mathbf{a}_2 + (l_3 - l_3')\mathbf{a}_3] \cdot \mathbf{q} = \begin{cases} 2m\pi \\ (2m+1)\pi \end{cases} \tag{4}$$

with integer m. If we introduce the reciprocal wavevectors $\mathbf{b}$ defined by

$$\mathbf{a}_i \cdot \mathbf{b}_j = 2\pi\delta_{ij} \tag{5}$$

and represent the wavevector $\mathbf{q}$ in this basis,

$$\mathbf{q} = \sum_i \xi_i \mathbf{b}_i = \xi\mathbf{b}_1 + \eta\mathbf{b}_2 + \zeta\mathbf{b}_3, \qquad \mathbf{a}_i \cdot \mathbf{q} = 2\pi\xi_i, \tag{6}$$

then the plane is given by

$$(l_1 - l_1')\xi + (l_2 - l_2')\eta + (l_3 - l_3')\zeta = \begin{cases} m \\ m + \frac{1}{2}. \end{cases} \tag{7}$$

But there are also cases where the factor has a more complex form, which yields a winding surface or a winding line. Such a surface appears in HP tridymite, equation (53). Lines of RUMs are planar, if they come from a factor of type (3) of the real or imaginary part. If the factors of both the real and the imaginary part are of type (3) then the line of RUMs is straight. If none of these factors are of this type, then the lines are generically non-planar, as in α-quartz (figure 6).

2.2. Basic equations

Suppose the oxygens are located at

$$\mathbf{r}_{\mathbf{n},i} = \mathbf{R}_{\mathbf{n},i} + \mathbf{u}_{\mathbf{n},i}, \tag{8}$$

$$\mathbf{R}_{\mathbf{n},i} = \sum_\alpha (n_\alpha + c_{i\alpha})\mathbf{a}_\alpha = \mathcal{A}(\mathbf{n} + \mathbf{c}_i) \tag{9}$$

with the equilibrium positions $\mathbf{R}$ and the displacements $\mathbf{u}$. The integers n_α number the elementary cells. The atomic coordinates of the $2n_t$ oxygens in the elementary cell are denoted by $c_{i,\alpha}$. The operator $\mathcal{A}$ maps the unit cube onto the elementary cell. It performs the similarity transformation

$$\mathcal{A}\mathbf{x} = \sum_\alpha \mathbf{a}_\alpha(\mathbf{e}_\alpha \cdot \mathbf{x}), \tag{10}$$

from the orthogonal unit vectors $\mathbf{e}_\alpha$ to the lattice vectors $\mathbf{a}_\alpha$. Thus the components of $\mathbf{x}$ and $\mathbf{n} + \mathbf{c}$ expand the vectors in the basis $\{\mathbf{a}\}$. The distance between the oxygens at the corners of the tetrahedra should be fixed to first order in the displacements. Thus for such a pair of atoms at $\mathbf{r}_{\mathbf{n}+\mathbf{m},i}$ and $\mathbf{r}_{\mathbf{n}+\mathbf{m}',j}$ with fixed distance one obtains the condition

$$(\mathbf{R}_{\mathbf{n}+\mathbf{m},i} - \mathbf{R}_{\mathbf{n}+\mathbf{m}',j}) \cdot (\mathbf{u}_{\mathbf{n}+\mathbf{m},i} - \mathbf{u}_{\mathbf{n}+\mathbf{m}',j}) = 0. \tag{11}$$

The distance vector reads

$$\mathbf{R}_{\mathbf{n}+\mathbf{m},i} - \mathbf{R}_{\mathbf{n}+\mathbf{m}',j} = \mathcal{A}\mathbf{d}_{\mathbf{m}-\mathbf{m}',i,j}, \tag{12}$$

$$\mathbf{d}_{\mathbf{m}-\mathbf{m}',i,j} = \mathbf{c}_i + \mathbf{m} - \mathbf{m}' - \mathbf{c}_j. \tag{13}$$

Thus equation (11) can be rewritten

$$\begin{aligned}\mathcal{A}\mathbf{d}_{\mathbf{m}-\mathbf{m}',i,j} \cdot (\mathbf{u}_{\mathbf{n}+\mathbf{m},i} - \mathbf{u}_{\mathbf{n}+\mathbf{m}',j}) &= \mathbf{d}_{\mathbf{m}-\mathbf{m}',i,j} \cdot (\mathcal{A}^{\mathrm{T}}\mathbf{u}_{\mathbf{n}+\mathbf{m},i} - \mathcal{A}^{\mathrm{T}}\mathbf{u}_{\mathbf{n}+\mathbf{m}',j}) \\ &= \mathbf{d}_{\mathbf{m}-\mathbf{m}',i,j} \cdot (\tilde{\mathbf{u}}_{\mathbf{n}+\mathbf{m},i} - \tilde{\mathbf{u}}_{\mathbf{n}+\mathbf{m}',j}) = 0,\end{aligned} \tag{14}$$

where $\mathcal{A}^{\mathrm{T}}$ is the transposed operator of $\mathcal{A}$,

$$\tilde{\mathbf{u}} := \mathcal{A}^{\mathrm{T}}\mathbf{u} = \sum_{\alpha} \mathbf{e}_\alpha (\mathbf{a}_\alpha \cdot \mathbf{u}). \tag{15}$$

The operator $\mathcal{A}^{\mathrm{T}}$ allows one to express

$$\mathcal{A}^{\mathrm{T}}\mathbf{b}_\alpha = 2\pi\mathbf{e}_\alpha, \qquad \mathcal{A}^{\mathrm{T}}\mathbf{q} = 2\pi\boldsymbol{\xi}. \tag{16}$$

Since the vector $\mathbf{d}$ is independent of $\mathbf{n}$, the Fourier transform of equation (14) yields

$$\mathbf{d}_{\mathbf{m}-\mathbf{m}',i,j} \cdot (\rho_{\mathbf{m}}\tilde{\mathbf{u}}_i(\mathbf{q}) - \rho_{\mathbf{m}'}\tilde{\mathbf{u}}_j(\mathbf{q})) = 0 \tag{17}$$

with

$$\rho_{\mathbf{m}} = \prod_{k=1}^{3} \rho_k^{m_k}, \tag{18}$$

$$\tilde{\mathbf{u}}_i(\mathbf{q}) = \sum_{\mathbf{n}} \exp\left(-\mathrm{i}\sum_k n_k \mathbf{a}_k \cdot \mathbf{q}\right)\tilde{\mathbf{u}}_{\mathbf{n},i}. \tag{19}$$

Equation (17) constitutes a set of linear homogeneous equations for the displacements $\mathbf{u}$. We are looking for those wavevectors $\mathbf{q}$ which allow non-trivial solutions of the set of equations (17). Note that $\mathcal{A}$ has disappeared from equation (17). Thus the lattice parameters of the unit cell do not enter into the calculation. Nevertheless, inversion symmetry and rotational symmetries play still a role. To facilitate notation the $6n_{\mathrm{t}}$ edges of the n_{t} tetrahedra are numbered by e. The edge e connects the vertices i_e and j_e. To this edge the triples $\mathbf{m}_e$, $\mathbf{m}'_e$ and the distance vector $\mathbf{d}_e = \mathbf{d}_{\mathbf{m}_e-\mathbf{m}'_e,i_e,j_e}$ are associated. Then equation (17) can be written as

$$\Delta_e := \mathbf{d}_e \cdot (\rho_{\mathbf{m}_e}\tilde{\mathbf{u}}_{i_e}(\mathbf{q}) - \rho_{\mathbf{m}'_e}\tilde{\mathbf{u}}_{j_e}(\mathbf{q})) = 0. \tag{20}$$

This set of homogeneous equations in the elongations $\mathbf{u}$ has non-trivial solutions, if the determinant $\mathcal{M}$ of the matrix M with $6n_{\mathrm{t}} \times 6n_{\mathrm{t}}$ elements

$$M_{e,k\alpha} = \frac{\partial\Delta_e}{\partial\tilde{u}_{k\alpha}} = d_{e\alpha}\left(\rho_{\mathbf{m}_e}\delta_{i_e,k} - \rho_{\mathbf{m}'_e}\delta_{j_e,k}\right) \tag{21}$$

vanishes. The index e of the edges denotes the rows; the indices k and α run independently from 1 to $2n_{\mathrm{t}}$ and from 1 to 3, respectively, and number the columns of the matrix.

In general the determinant of M yields a complex number as a function of the ρ_k. Thus both the real part and the imaginary part of $\mathcal{M}$ have to vanish. The determinant can be expanded:

$$\mathcal{M} := \det(M) = \sum_{ijk} \mu_{ijk}\rho_1^i\rho_2^j\rho_3^k \tag{22}$$

with real coefficients μ_{ijk} and integer i, j, k. Thus $\mathcal{M}(\rho_1^*, \rho_2^*, \rho_3^*) = \mathcal{M}^*(\rho_1, \rho_2, \rho_3)$ holds. Therefore a vanishing $\mathcal{M}$ for some wavevector $\mathbf{q}$ also implies that it vanishes for $-\mathbf{q}$.

2.3. Inversion symmetry

We show that in the case of inversion symmetry $\mathcal{M}$ multiplied by an appropriate factor $\rho_{\mathbf{m}}$ is real. Suppose that the centre of inversion is located at

$$\mathbf{R}_{\mathrm{I}} = \mathcal{A}\mathbf{p} = \sum_{\alpha} p^{\alpha}\mathbf{a}_{\alpha} \tag{23}$$

and denote the sublattice obtained by inversion from the sublattice i by $I(i)$. (i may, but need not, be identical to $I(i)$). Then

$$\mathbf{c}_i + \mathbf{c}_{I(i)} = 2\mathbf{p} + \mathbf{l}_i \tag{24}$$

holds with integer $l_i^{\alpha} = l_{I(i)}^{\alpha}$. Inversion is also applied to the edges, which generates $I(e)$ from e. Then the corners at the ends of the edges obey

$$i_{I(e)} = I(i_e), \qquad j_{I(e)} = I(j_e). \tag{25}$$

Due to this inversion the two distance vectors add up to zero,

$$\mathbf{d}_e + \mathbf{d}_{I(e)} = \mathbf{0} \tag{26}$$

with

$$\mathbf{d}_e = \mathbf{c}_{i_e} + \mathbf{m}_e - \mathbf{m}'_e - \mathbf{c}_{j_e}, \tag{27}$$

$$\mathbf{d}_{I(e)} = \mathbf{c}_{I(i_e)} + \mathbf{m}_{I(e)} - \mathbf{m}'_{I(e)} - \mathbf{c}_{I(j_e)}. \tag{28}$$

Therefore one obtains

$$\mathbf{s}_e := \mathbf{m}_e + \mathbf{m}_{I(e)} + \mathbf{l}_{i_e} = \mathbf{m}'_e + \mathbf{m}'_{I(e)} + \mathbf{l}_{j_e}, \tag{29}$$

which yields

$$\tilde{\mathbf{m}}_e + \tilde{\mathbf{m}}_{I(e)} = \mathbf{0} \tag{30}$$

with

$$\tilde{\mathbf{m}}_e = \mathbf{m}_e + \frac{\mathbf{l}_{i_e} - \mathbf{s}_e}{2}, \qquad \tilde{\mathbf{m}}_{I(e)} = \mathbf{m}_{I(e)} + \frac{\mathbf{l}_{i_e} - \mathbf{s}_e}{2}. \tag{31}$$

The matrix $\tilde{M}$ is introduced by

$$M_{e,k\alpha} = \rho_{\mathbf{s}_e/2}\rho_{-\mathbf{l}_k/2}\tilde{M}_{e,k\alpha}, \tag{32}$$

$$\tilde{M}_{e,k\alpha} = d_{e\alpha}\left(\rho_{\tilde{\mathbf{m}}_e}\delta_{i_e,k} - \rho_{\tilde{\mathbf{m}}'_e}\delta_{j_e,k}\right). \tag{33}$$

In rows e and $I(e)$ the only non-zero matrix elements of $\tilde{M}$ are

$$\tilde{M}_{e,i_e\alpha} = d_{e\alpha}\rho_{\tilde{\mathbf{m}}_e}, \qquad \tilde{M}_{e,j_e\alpha} = -d_{e\alpha}\rho_{\tilde{\mathbf{m}}'_e}, \tag{34}$$

$$\tilde{M}_{I(e),i_e\alpha} = d_{e\alpha}\rho_{-\tilde{\mathbf{m}}_e} = \tilde{M}^*_{e,i_e\alpha}, \qquad \tilde{M}_{I(e),j_e\alpha} = -d_{e\alpha}\rho_{-\tilde{\mathbf{m}}'_e} = \tilde{M}^*_{e,j_e\alpha}. \tag{35}$$

Therefore exchanging all pairs of rows e and $I(e)$ will transform the determinant $\tilde{\mathcal{M}}$ into $(-)^{3n_{\mathrm{t}}}$ times the determinant in which all arguments ρ_i are replaced by $1/\rho_i$ (note that $\rho_{-\mathbf{m}} = 1/\rho_{\mathbf{m}}$). Since a tetrahedron does not transform into itself under inversion, inversion symmetry is only possible for even n_{t}. Thus

$$\tilde{\mathcal{M}}(\rho_1, \rho_2, \rho_3) = \tilde{\mathcal{M}}\left(\frac{1}{\rho_1}, \frac{1}{\rho_2}, \frac{1}{\rho_3}\right). \tag{36}$$

Since for real wavevectors $\mathbf{q}$ one has $1/\rho_i = \rho_i^*$, one deduces

$$\tilde{\mathcal{M}} = \tilde{\mathcal{M}}^*. \tag{37}$$

Thus $\tilde{\mathcal{M}}$ is real for crystals with inversion symmetry. The connection between $\tilde{\mathcal{M}}$ and $\mathcal{M}$ is obtained from equations (31) and (32):

$$\tilde{\mathcal{M}} := \det(\tilde{M}) = (\rho_{\Sigma\mathbf{m}})^{-3/2}\mathcal{M}, \tag{38}$$

$$(\rho_{\Sigma\mathbf{m}})^{-3/2} = \prod_e (\rho_{\mathbf{s}_e})^{-1/2} \prod_i (\rho_{\mathbf{l}_i})^{3/2}. \tag{39}$$

The sum $\sum \mathbf{m}$ has to be extended over all vertices of all tetrahedra. Since each vertex belongs to two tetrahedra, there are two contributions to each vertex.

Although relation (36) holds for crystals with inversion centre only, the transformation from $\mathcal{M}$ to $\tilde{\mathcal{M}}$ is also useful for lattices without inversion symmetry for the following reason: the introduction of the $\mathbf{m}$ is to some extent arbitrary. One may add an arbitrary $\mathbf{m}_c$ to $\mathbf{m}$ at all corners of a given tetrahedron without changing the distance vectors $\mathbf{d}$, $\mathbf{m}' = \mathbf{m} + \mathbf{m}_c$. Then in all six rows for the edges of this tetrahedron an extra factor $\rho_{\mathbf{m}_c}$ appears, $\mathcal{M}' = \rho_{\mathbf{m}_c}^6 \mathcal{M}$. Then one obtains $\sum \mathbf{m}' = \sum \mathbf{m} + 4\mathbf{m}_c$ and $\tilde{\mathcal{M}}' = \tilde{\mathcal{M}}$. Therefore $\tilde{\mathcal{M}}$ is invariant against this arbitrary choice in contrast to $\mathcal{M}$. The overall sign of $\tilde{\mathcal{M}}$ depends on the sequence of the vertices. Thus it is arbitrary.

As a consequence, crystals with inversion symmetry will show areas for RUMs in reciprocal space, since only one condition has to be fulfilled. If inversion symmetry is lacking, then both the real and the imaginary parts of $\tilde{\mathcal{M}}$ have to vanish. Unless both conditions coincide for whole areas, one obtains only lines for RUMs in reciprocal space.

2.4. Remarks on the calculation

The calculation is performed by means of the algebraic computer program MAPLE. If the lattice is without an inversion centre, then $\tilde{\mathcal{M}}$ is decomposed into its real part $\mathcal{R}_1$ and its imaginary part $\mathcal{R}_2$. If besides the three factors ρ_k there are no other variables, then the calculation of the determinant is extremely fast. If there is one extra variable like x in β-quartz then it takes a few seconds. If there are three variables, like x_2, y_2, and z_2 in α-cristobalite and in α-quartz, then it takes up to the order of hours. However, if one assigns rational fractions like $x_2 = 239\,76/100\,000$, then it runs very quickly, whereas it takes quite a while if one chooses decimal fractions like $x_2 = 0.239\,76$. Apparently the exact calculation facilitates the calculation of the determinant, although it produces fractions with numerators and denominators of enormous size. Then also factorization still works, whereas it does not for decimal fractions due to rounding errors.

The degeneracy of the modes can easily be calculated for RUMs on planes or on straight lines by determining the rank of the matrix $\tilde{\mathcal{M}}$, since the corresponding restriction can easily be evaluated. If the surfaces or lines are bent, then this is more difficult, since the constrained ρ_k have to be given explicitly. In the following we will not determine the degeneracies.

The crystallographic data used here are those of [12]. They describe average atomic positions, which are not necessarily the same as the instantaneous local structure. Indeed the average positions are inconsistent with pair distribution functions [13]. This obviously is due to the RUMs. Thus the present analysis gives the RUM spectrum of the average structure.

To the extent that the location of the RUMs is given by symmetry, there will be obvious agreement between those determined in [1–3] and ours. For bent lines many agreements will be found. In comparison three things have to be kept in mind. First of all the cited references give only graphical representations. Therefore comparison is made by appearance only. Secondly, unless the atomic coordinates are determined by symmetry, theirs may differ from the ones used here. Thirdly, apparently Dove *et al* have included quasi-RUMs, that is regions in reciprocal space with a low phonon frequency, whereas here only zero-frequency modes are taken into account.

3. Various SiO_2 crystals

In the following, the RUMs for five polymorphs of SiO_2 crystals are determined.

3.1. β-cristobalite

The coordinates c' for the Si ions and c for the O ions are given by

i	$c'_{i,1}$	$c'_{i,2}$	$c'_{i,3}$
1	1/8	1/8	1/8
2	−1/8	−1/8	−1/8

i	$c_{i,1}$	$c_{i,2}$	$c_{i,3}$
1	0	0	0
2	1/2	0	0
3	0	1/2	0
4	0	0	1/2

$$\mathbf{a}_1 = \tfrac{a}{2}\mathbf{e}_2 + \tfrac{a}{2}\mathbf{e}_3 \qquad \mathbf{a}_2 = \tfrac{a}{2}\mathbf{e}_1 + \tfrac{a}{2}\mathbf{e}_3 \qquad \mathbf{a}_3 = \tfrac{a}{2}\mathbf{e}_1 + \tfrac{a}{2}\mathbf{e}_2. \tag{40}$$

The corners of the two tetrahedra are obtained by applying $\mathcal{A}$ to
the first tetrahedron: $\mathbf{c}_1, \mathbf{c}_2, \mathbf{c}_3, \mathbf{c}_4$; and
the second tetrahedron: $\mathbf{c}_1, \mathbf{c}_2 - \mathbf{e}_1, \mathbf{c}_3 - \mathbf{e}_2, \mathbf{c}_4 - \mathbf{e}_3$.
The determinant evaluates to

$$\tilde{\mathcal{M}} = \frac{(1-\rho_1)(1-\rho_2)(1-\rho_3)(\rho_1-\rho_2)(\rho_1-\rho_3)(\rho_2-\rho_3)}{2^{12}\rho_1^{3/2}\rho_2^{3/2}\rho_3^{3/2}}. \tag{41}$$

With equation (6) one obtains

$$\frac{1-\rho_k}{\rho_k^{1/2}} = -2\mathrm{i}\sin(\mathbf{a}_k\mathbf{q}/2) = -2\mathrm{i}\sin(\pi\xi_k), \tag{42}$$

$$\frac{\rho_k-\rho_l}{(\rho_k\rho_l)^{1/2}} = 2\mathrm{i}\sin((\mathbf{a}_k-\mathbf{a}_l)\mathbf{q}/2) = 2\mathrm{i}\sin(\pi(\xi_k-\xi_l)). \tag{43}$$

Thus all RUMs are located in the planes in reciprocal space

$$(0,\eta,\zeta), \quad (\xi,0,\zeta), \quad (\xi,\eta,0), \quad (\xi,\xi,\zeta), \quad (\xi,\eta,\xi), \quad (\xi,\eta,\eta). \tag{44}$$

The crystal has a centre of inversion. One easily checks equation (36) for this crystal.

Comparison. The planes of RUMs found agree completely with those given in [1].

3.2. HP tridymite

The atomic coordinates of the HP tridymite phase of SiO_2 are given by

i	$c'_{i,1}$	$c'_{i,2}$	$c'_{i,3}$
1	1/3	2/3	z
2	2/3	1/3	$-z$
3	2/3	1/3	$1/2+z$
4	1/3	2/3	$1/2-z$

i	$c_{i,1}$	$c_{i,2}$	$c_{i,3}$
1	1/3	2/3	1/4
2	2/3	1/3	3/4
3	1/2	0	0
4	0	1/2	0
5	1/2	1/2	0
6	1/2	0	1/2
7	0	1/2	1/2
8	1/2	1/2	1/2

$$\mathbf{a}_1 = \tfrac{1}{2}a\mathbf{e}_1 - \tfrac{\sqrt{3}}{2}a\mathbf{e}_2 \qquad \mathbf{a}_2 = \tfrac{1}{2}a\mathbf{e}_1 + \tfrac{\sqrt{3}}{2}a\mathbf{e}_2 \qquad \mathbf{a}_3 = c\mathbf{e}_3. \tag{45}$$

Equation (17) has to be fulfilled for the edges of the four tetrahedra with corners obtained by applying $\mathcal{A}$ to
the first tetrahedron: $\mathbf{c}_1, \mathbf{c}_3 + \mathbf{e}_2, \mathbf{c}_4, \mathbf{c}_5$;
the second tetrahedron: $\mathbf{c}_2 - \mathbf{e}_3, \mathbf{c}_3, \mathbf{c}_4 + \mathbf{e}_1, \mathbf{c}_5$;

the third tetrahedron: $\mathbf{c}_2$, $\mathbf{c}_6$, $\mathbf{c}_7 + \mathbf{e}_1$, $\mathbf{c}_8$; and
the fourth tetrahedron: $\mathbf{c}_1$, $\mathbf{c}_6 + \mathbf{e}_2$, $\mathbf{c}_7$, $\mathbf{c}_8$.
The determinant $\tilde{\mathcal{M}}$ yields

$$\tilde{\mathcal{M}} = f_2^2(\rho_1, \rho_2)\frac{(1-\rho_3)}{2^{32}3^2\rho_3^{1/2}}\mathcal{R}, \tag{46}$$

$$\mathcal{R} = 9\left(\rho_3 + \frac{1}{\rho_3}\right) - 4f_1(\rho_1, \rho_2) + 14, \tag{47}$$

$$\begin{aligned} f_1(\rho_1, \rho_2) &= \frac{(1+\rho_1)(1+\rho_2)(1+\rho_1\rho_2)}{\rho_1\rho_2} \\ &= 8\cos(\mathbf{a}_1\mathbf{q}/2)\cos(\mathbf{a}_2\mathbf{q}/2)\cos((\mathbf{a}_1+\mathbf{a}_2)\mathbf{q}/2) \\ &= 2(1+\cos(\mathbf{a}_1\mathbf{q}) + \cos(\mathbf{a}_2\mathbf{q}) + \cos((\mathbf{a}_1+\mathbf{a}_2)\mathbf{q})), \end{aligned} \tag{48}$$

$$\begin{aligned} f_2(\rho_1, \rho_2) &= \frac{(1-\rho_1)(1-\rho_2)(1-\rho_1\rho_2)}{\rho_1\rho_2} \\ &= 8\mathrm{i}\sin(\mathbf{a}_1\mathbf{q}/2)\sin(\mathbf{a}_2\mathbf{q}/2)\sin((\mathbf{a}_1+\mathbf{a}_2)\mathbf{q}/2) \\ &= 2\mathrm{i}(\sin(\mathbf{a}_1\mathbf{q}) + \sin(\mathbf{a}_2\mathbf{q}) - \sin((\mathbf{a}_1+\mathbf{a}_2)\mathbf{q})). \end{aligned} \tag{49}$$

These functions, f_1 and f_2, as well as the later introduced functions f_3, equation (65), and f_4, equation (108), are invariant under rotations by $2\pi/3$ around the z-axis, which causes the following transformation

$$\begin{aligned} &\mathbf{a}_1 \to \mathbf{a}_2 \to -\mathbf{a}_1 - \mathbf{a}_2 \to \mathbf{a}_1, \\ &\rho_1 \to \rho_2 \to 1/(\rho_1\rho_2) \to \rho_1. \end{aligned} \tag{50}$$

Due to the factor $1-\rho_3$ in equation (46) RUMs are located in the plane

$$(\xi, \eta, 0). \tag{51}$$

The factors of f_2 yield RUMs in the planes

$$(0, \eta, \zeta), \qquad (\xi, 0, \zeta), \qquad (\xi, -\xi, \zeta). \tag{52}$$

In contrast, the zeros of $\mathcal{R}$ describe a winding surface in reciprocal space, which may be written as

$$\begin{aligned} \cos(2\pi\zeta) &= \tfrac{16}{9}\cos(\pi\xi)\cos(\pi\eta)\cos(\pi(\xi+\eta)) - \tfrac{7}{9} \\ &= \tfrac{4}{9}(\cos(2\pi\xi) + \cos(2\pi\eta) + \cos(2\pi(\xi+\eta))) - \tfrac{1}{3}. \end{aligned} \tag{53}$$

Note that the maximum of the sum of the right-hand side (rhs) is $+1$, which is obtained at $[0, 0, 0]$. The minimum of the rhs is -1, which is reached at $[\pm 1/3, \pm 1/3, 1/2]$. For $\xi = 1/2$ or $\eta = 1/2$ or $\xi + \eta = 1/2$ one obtains $\cos(2\pi\zeta) = -7/9$, which yields $\zeta = l = \pm 0.391\,83$.

Comparison. These results are in full agreement with those obtained by Dove *et al* [11] by means of their numerical CRUSH program [7, 8] and reported in [1].

Other derivation. One may determine this bending RUM also in the following way. One starts with the equations for the edges between $\mathbf{c}_3$, $\mathbf{c}_4$, and $\mathbf{c}_5$. Since they all lie in the xy-plane, the third component does not enter, and one obtains the equations

$$\begin{aligned} &\tilde{u}_{4,1} = \tilde{u}_{5,1}, \qquad \rho_1\tilde{u}_{4,1} = \tilde{u}_{5,1}, \\ &\tilde{u}_{3,2} = \tilde{u}_{5,2}, \qquad \rho_2\tilde{u}_{3,2} = \tilde{u}_{5,2}, \\ &\rho_2(\tilde{u}_{3,1} + \tilde{u}_{3,2}) = \tilde{u}_{4,1} + \tilde{u}_{4,2}, \qquad \tilde{u}_{3,1} + \tilde{u}_{3,2} = \rho_1(\tilde{u}_{4,1} + \tilde{u}_{4,2}). \end{aligned} \tag{54}$$

Evidently, if

$$\rho_1 \neq 1, \qquad \rho_2 \neq 1, \qquad \rho_1\rho_2 \neq 1, \tag{55}$$

then all these components vanish:

$$\tilde{u}_{3,1} = \tilde{u}_{3,2} = \tilde{u}_{4,1} = \tilde{u}_{4,2} = \tilde{u}_{5,1} = \tilde{u}_{5,2} = 0. \tag{56}$$

Similarly one shows by considering the third and fourth tetrahedra that under the same condition (55) one obtains

$$\tilde{u}_{6,1} = \tilde{u}_{6,2} = \tilde{u}_{7,1} = \tilde{u}_{7,2} = \tilde{u}_{8,1} = \tilde{u}_{8,2} = 0. \tag{57}$$

This implies that the tetrahedra are rotated around axes parallel to the xy-plane. There are 12 equations left for the 12 other components $\tilde{u}$. One can use six of them to eliminate $\tilde{u}_{3,3}$ to $\tilde{u}_{8,3}$. Finally, one calculates the determinant of the coefficient matrix

$$\begin{pmatrix}
-\frac{\rho_3}{6\rho_2} & -\frac{\rho_3}{3\rho_2} & \frac{\rho_3}{4\rho_2} & \frac{1}{6} & \frac{1}{3} & -\frac{1}{4} \\
\frac{\rho_1\rho_3}{3} & \frac{\rho_1\rho_3}{6} & \frac{\rho_1\rho_3}{4} & -\frac{1}{3} & -\frac{1}{6} & -\frac{1}{4} \\
-\frac{\rho_3}{6} & \frac{\rho_3}{6} & \frac{\rho_3}{4} & \frac{1}{6} & -\frac{1}{6} & -\frac{1}{4} \\
-\frac{1}{6\rho_2} & -\frac{1}{3\rho_2} & -\frac{1}{4\rho_2} & \frac{1}{6} & \frac{1}{3} & \frac{1}{4} \\
\frac{\rho_1}{3} & \frac{\rho_1}{6} & -\frac{\rho_1}{4} & -\frac{1}{3} & -\frac{1}{6} & \frac{1}{4} \\
-\frac{1}{6} & \frac{1}{6} & -\frac{1}{4} & \frac{1}{6} & -\frac{1}{6} & \frac{1}{4}
\end{pmatrix} \tag{58}$$

of the last six equations for the six components of $\tilde{\mathbf{u}}_1$ and $\tilde{\mathbf{u}}_2$, which has to vanish. This determinant factorizes in factors $\rho_3 - 1$ and

$$\begin{aligned} 2\left(\frac{1}{\rho_1} + \rho_1 + \frac{1}{\rho_2} + \rho_2 + \frac{1}{\rho_1\rho_2} + \rho_1\rho_2\right) - \frac{9}{2}\left(\frac{1}{\rho_3} + \rho_3\right) - 3 \\ = 4(\cos(\mathbf{a}_1\mathbf{q}) + \cos(\mathbf{a}_2\mathbf{q}) + \cos((\mathbf{a}_1 + \mathbf{a}_2)\mathbf{q})) - 9\cos(\mathbf{a}_3\mathbf{q}) - 3 = 0, \end{aligned} \tag{59}$$

which again yields equation (53).

3.3. β-quartz

The coordinates for the Si and O ions are given by

i	$c'_{i,1}$	$c'_{i,2}$	$c'_{i,3}$
1	1/2	0	0
2	0	1/2	2/3
3	1/2	1/2	1/3

i	$c_{i,1}$	$c_{i,2}$	$c_{i,3}$
1	x	$2x$	1/2
2	$-2x$	$-x$	1/6
3	x	$-x$	5/6
4	$-x$	$-2x$	1/2
5	$2x$	x	1/6
6	$-x$	x	5/6

$$\begin{aligned} \mathbf{a}_1 &= \tfrac{1}{2}a\mathbf{e}_1 - \tfrac{\sqrt{3}}{2}a\mathbf{e}_2 \\ \mathbf{a}_2 &= \tfrac{1}{2}a\mathbf{e}_1 + \tfrac{\sqrt{3}}{2}a\mathbf{e}_2 \\ \mathbf{a}_3 &= c\mathbf{e}_3. \end{aligned} \tag{60}$$

The corners of the three tetrahedra are obtained by applying $\mathcal{A}$ to
the first tetrahedron: $\mathbf{c}_2 + \mathbf{e}_1$, $\mathbf{c}_3 - \mathbf{e}_3$, $\mathbf{c}_5$, $\mathbf{c}_6 + \mathbf{e}_1 - \mathbf{e}_3$;
the second tetrahedron: $\mathbf{c}_1$, $\mathbf{c}_3 + \mathbf{e}_2$, $\mathbf{c}_4 + \mathbf{e}_2$, $\mathbf{c}_6$; and
the third tetrahedron: $\mathbf{c}_1$, $\mathbf{c}_2 + \mathbf{e}_1 + \mathbf{e}_2$, $\mathbf{c}_4 + \mathbf{e}_1 + \mathbf{e}_2$, $\mathbf{c}_5$.
The determinant reads

$$\tilde{\mathcal{M}} = \left(\frac{4x(3x-1)}{9}\right)^3 \frac{1-\rho_3}{\rho_3^{1/2}} (\mathcal{R}_1 + \mathcal{R}_2), \tag{61}$$

$$\mathcal{R}_1 = \frac{1+\rho_3}{\rho_3^{1/2}} f_2(\rho_1, \rho_2) \left(-k_3^3\left(\frac{1+\rho_3^2}{\rho_3}\right) + k_1 + k_2 f_1(\rho_1, \rho_2)\right), \tag{62}$$

$$\mathcal{R}_2 = 2x(2x-1)(3x-1)(4x-1)(6x-1)\frac{1-\rho_3}{\rho_3^{1/2}} f_3(\rho_1, \rho_2), \tag{63}$$

$$f_3(\rho_1, \rho_2) = \frac{(\rho_1-\rho_2)(1-\rho_1\rho_2^2)(1-\rho_1^2\rho_2)}{\rho_1^2\rho_2^2}, \tag{64}$$

$$k_1 = 2x(4x-1)(432x^4 - 540x^3 + 252x^2 - 51x + 4), \tag{65}$$

$$k_2 = -x(4x-1)(3x-1)^2, \tag{66}$$

$$k_3 = 12x^2 - 6x + 1. \tag{67}$$

Due to the factor $(1-\rho_3)$, RUMs are obtained in the plane

$$(\xi, \eta, 0). \tag{68}$$

The factor $(1+\rho_3)$ in $\mathcal{R}_1$ and the zeros of f_3 in $\mathcal{R}_2$ yield RUMs along the straight lines

$$[\xi, \xi, 1/2], \qquad [\xi, -2\xi, 1/2], \qquad [-2\xi, \xi, 1/2]. \tag{69}$$

The zeros of f_2 in $\mathcal{R}_1$ and of f_3 in $\mathcal{R}_2$ yield RUMs along the straight lines

$$[0, 0, \zeta], \qquad [0, 1/2, \zeta], \qquad [1/2, 0, \zeta], \qquad [1/2, 1/2, \zeta]. \tag{70}$$

Finally, the zeros of the term in the large parentheses in the expression for $\mathcal{R}_1$ and the zeros of f_3 in $\mathcal{R}_2$ yield RUMs along the curves

$$[\xi, \xi, \zeta(\xi)], \qquad [\xi, -2\xi, \zeta(\xi)], \qquad [-2\xi, \xi, \zeta(\xi)], \tag{71}$$

where $\zeta(\xi)$ is given by

$$\cos(2\pi\zeta(\xi)) = \frac{k_1 + 8k_2\cos^2(\pi\xi)\cos(2\pi\xi)}{2k_3^3}. \tag{72}$$

With $x = 0.4202$ of [12] one obtains

$$k_1 = 0.267\,99, \qquad k_2 = -0.019\,427, \qquad k_3 = 0.597\,62 \tag{73}$$

and

$$\cos(2\pi\zeta(\xi)) = 0.6278 - 0.3641\cos^2(\pi\xi)\cos(2\pi\xi). \tag{74}$$

However, this value of x yields tetrahedra which are far from being equilateral. The value for equilateral tetrahedra is[1]

$$x = \frac{1}{2} - \frac{1}{\sqrt{12}} = 0.2113, \tag{75}$$

which yields

$$k_1 = -0.015\,801, \qquad k_2 = 0.004\,380, \qquad k_3 = 0.267\,95, \tag{76}$$

$$\cos(2\pi\zeta(\xi)) = -0.410\,68 + 0.910\,68\cos^2(\pi\xi)\cos(2\pi\xi). \tag{77}$$

The function $\zeta(\xi)$ is plotted for both values of x in figure 1.

Comparison. We find agreement of the RUMs for β-quartz in reciprocal space with those given in [11, 1–3]. This includes the winding lines of figure 1 seen in [2, 3] with the ideal value x of equation (75).

[1] The maintainers of the pages of [12] have been informed on this discrepancy and a correction has been suggested.

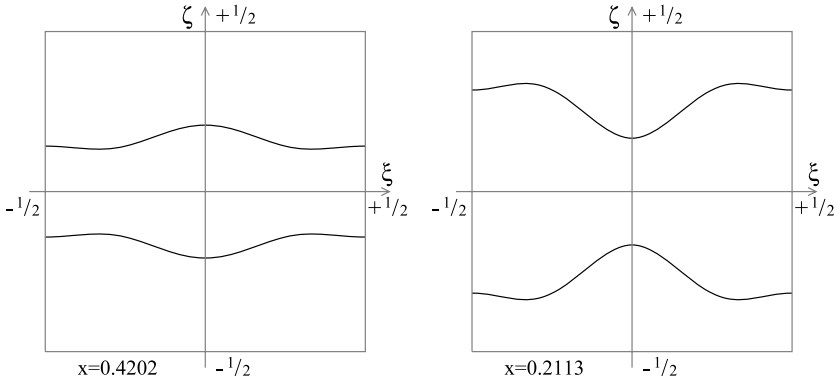

Figure 1. $\zeta(\xi)$ of the RUMs of β-quartz given by equations (71) and (72) for $x = 0.4202$ and 0.2113.

3.4. α-cristobalite

The coordinates c' for the Si ions and c for the O ions are given by

i	$c'_{i,1}$	$c'_{i,2}$	$c'_{i,3}$
1	x_1	x_1	0
2	$-x_1$	$-x_1$	1/2
3	$1/2-x_1$	$1/2+x_1$	1/4
4	$1/2+x_1$	$1/2-x_1$	3/4

i	$c_{i,1}$	$c_{i,2}$	$c_{i,3}$
1	x_2	y_2	z_2
2	$-x_2$	$-y_2$	$1/2+z_2$
3	$1/2-y_2$	$1/2+x_2$	$1/4+z_2$
4	$1/2+y_2$	$1/2-x_2$	$3/4+z_2$
5	y_2	x_2	$-z_2$
6	$-y_2$	$-x_2$	$1/2-z_2$
7	$1/2-x_2$	$1/2+y_2$	$1/4-z_2$
8	$1/2+x_2$	$1/2-y_2$	$3/4-z_2$

$\mathbf{a}_1 = a\mathbf{e}_1$
$\mathbf{a}_2 = a\mathbf{e}_2$
$\mathbf{a}_3 = c\mathbf{e}_3$. (78)

The corners of the four tetrahedra are obtained by applying $\mathcal{A}$ to
the first tetrahedron: $\mathbf{c}_1, \mathbf{c}_4 - \mathbf{e}_3, \mathbf{c}_5, \mathbf{c}_7$;
the second tetrahedron: $\mathbf{c}_2, \mathbf{c}_3 - \mathbf{e}_1 - \mathbf{e}_2, \mathbf{c}_6, \mathbf{c}_8 - \mathbf{e}_1 - \mathbf{e}_2$;
the third tetrahedron: $\mathbf{c}_1 + \mathbf{e}_2, \mathbf{c}_3, \mathbf{c}_6 + \mathbf{e}_2, \mathbf{c}_7$; and
the fourth tetrahedron: $\mathbf{c}_2 + \mathbf{e}_1, \mathbf{c}_4, \mathbf{c}_5 + \mathbf{e}_1 + \mathbf{e}_3, \mathbf{c}_8$.
The determinant reads

$$\tilde{\mathcal{M}} = k_0^4(\mathcal{R}_1 + \mathcal{R}_2), \tag{79}$$

$$\mathcal{R}_1 = \sum_{l=0}^{2} g_l \cos^l(2\pi\xi_3), \tag{80}$$

$$\mathcal{R}_2 = k' \frac{(1-\rho_1^2)(1-\rho_2^2)(1-\rho_3^2)(\rho_1-\rho_2)(1-\rho_1\rho_2)}{\rho_1^2\rho_2^2\rho_3}, \tag{81}$$

$$g_l = \sum_{ij} k_{ijl} \cos^i(2\pi\xi_1)\cos^j(2\pi\xi_2), \tag{82}$$

$$k_0 = \tfrac{1}{8}(2x_2-1)(8z_2y_2 + x_2 - y_2) \tag{83}$$

with

$$k_{ijl} = k_{jil}. \tag{84}$$

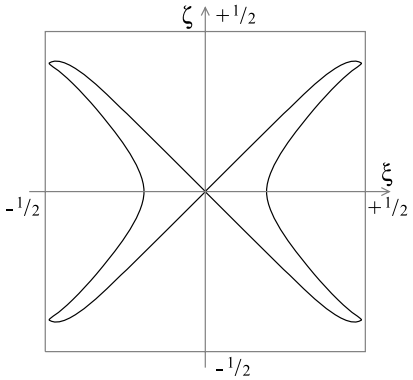

Figure 2. $\zeta(\xi)$ of the RUMs of α-cristobalite described by equations (88)–(90).

The sum over i and j runs at most up to $i = 3$, $j = 3$, $i + j = 4$. The coefficients k_{ijl} are polynomials in x_2, y_2, z_2. They are of order 4 in z_2 and of order 8 in x_2 and y_2. Thus in general they are lengthy expressions.

For

$$x_2 = 0.239\,76, \qquad y_2 = 0.103\,24, \qquad z_2 = 0.178\,44 \tag{85}$$

from [12] one obtains

$$k' = -0.000\,527\,47, \qquad k_0 = -0.018\,470, \tag{86}$$

and the non-zero coefficients k_{ijl}

i	j	$100k_{ij0}$
0	0	−8.0953
0	1	9.6093
0	2	9.4540
0	3	−10.9503
1	1	−8.4081
1	2	−7.3564
1	3	7.9854

i	j	$100k_{ij1}$
0	0	−0.7104
0	1	−3.7422
0	2	2.5622
1	1	−19.5336
1	2	18.3067
2	2	−15.9707

i	j	$100k_{ij2}$
0	0	8.8057
0	1	−5.8672
1	1	3.9092.

(87)

The zeros $\rho_1 = \pm 1$, $\rho_2 = \pm 1$, $\rho_2 = \rho_1$, $\rho_2 = 1/\rho_1$ of $\mathcal{R}_2$ yield RUMs for the zeros of $\mathcal{R}_1$ from

$$\cos(2\pi\zeta(\xi)) = \frac{-g_1 \pm \sqrt{d}}{2g_2}, \qquad d = g_1^2 - 4g_0g_2. \tag{88}$$

For $\rho_1 = 1$ and $\rho_2 = 1$ one obtains RUMs along the lines

$$[0, \xi, \zeta(\xi)], \qquad [\xi, 0, \zeta(\xi)], \tag{89}$$

respectively, with

$$\begin{aligned} 10^2 g_2 &= 2.9385 - 1.9579\cos(2\pi\xi), \\ 10^2 g_1 &= -1.8904 - 4.9691\cos(2\pi\xi) + 4.8982\cos^2(2\pi\xi), \\ 10^4 d &= (1 - \cos(2\pi\xi))^2(3.3647 + 4.1431\cos(2\pi\xi) + 0.7718\cos^2(2\pi\xi)). \end{aligned} \tag{90}$$

They are shown in figure 2.

For $\rho_1 = -1$ and $\rho_2 = -1$ one obtains RUMs along the lines

$$[1/2, \xi, \zeta(\xi)], \qquad [\xi, 1/2, \zeta(\xi)] \tag{91}$$

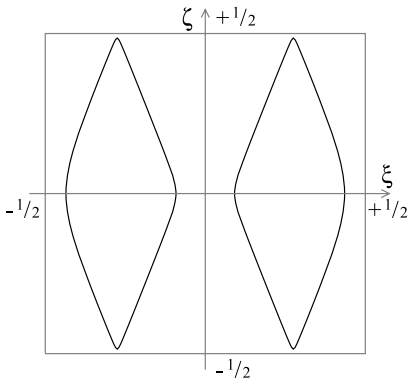

Figure 3. $\zeta(\xi)$ of the RUMs of α-cristobalite given by equations (93), (94) and (96).

respectively, with

$$\begin{aligned} 10^2 g_2 &= 14.6729 - 9.7764\cos(2\pi\xi), \\ 10^2 g_1 &= 5.5940 + 34.0981\cos(2\pi\xi) - 31.7152\cos^2(2\pi\xi), \\ 10^4 d &= -127.156 + 330.023\cos(2\pi\xi) - 74.142\cos^2(2\pi\xi) \\ &\quad - 394.118\cos^3(2\pi\xi) + 265.367\cos^4(2\pi\xi). \end{aligned} \tag{92}$$

The calculation with (85) did not give real solutions $\zeta(\xi)$.

For $\rho_2 = \rho_1$ and $1/\rho_1$ one obtains RUMs along the lines

$$[\xi, \xi, \zeta(\xi)], \qquad [\xi, -\xi, \zeta(\xi)] \tag{93}$$

with

$$\begin{aligned} 10^2 g_2 &= (2.9674 - 1.9772\cos(2\pi\xi))^2, \\ 10^2 g_1 &= -0.7104 - 7.4844\cos(2\pi\xi) - 14.4092\cos^2(2\pi\xi) \\ &\quad + 36.6135\cos^3(2\pi\xi) - 15.9707\cos^4(2\pi\xi), \\ d &= (2g_2 + g_1)^2. \end{aligned} \tag{94}$$

The square root of d is rational in this case. The first solution (88) yields the straight line of RUMs

$$[\xi, \pm\xi, 0]. \tag{95}$$

The second one yields the relation

$$\cos(2\pi\zeta(\xi)) = -1 - \frac{g_1}{g_2}. \tag{96}$$

The locations of these RUMs in reciprocal space are shown in figure 3.

The RUMs given by the zero $\rho_3 = 1$ are the RUMs from equation (95) just mentioned plus RUMs along the lines $[\xi, \eta, 0]$ with ξ and η related by

$$\cos(2\pi\xi)\cos(2\pi\eta) - A(\cos(2\pi\xi) + \cos(2\pi\eta)) + B = 0, \tag{97}$$

where for the above given x_2, y_2, z_2 one obtains

$$A = 1.3713, \qquad B = 1.5048. \tag{98}$$

The corresponding line is plotted in figure 4.

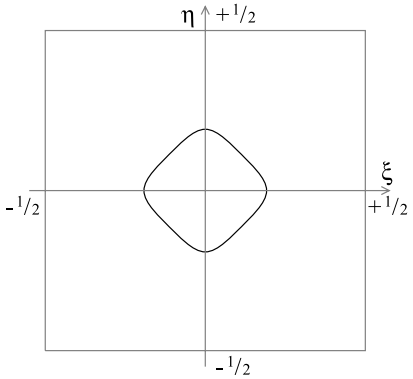

Figure 4. η versus ξ of the RUMs of α-cristobalite given by equations (97) and (98).

Finally, the RUMs given by the zero $\rho_3 = -1$ of $\mathcal{R}_2$ are given by the lines $[\xi, \eta, 1/2]$ with ξ and η related by

$$\sum_{i,j=0}^{3} k_{i,j} \cos^i(2\pi\xi) \cos^j(2\pi\eta) = 0, \tag{99}$$

which with (85) yields

$$\begin{aligned} 15.9707 \cos^2(2\pi\xi) \cos^2(2\pi\eta) + \; & 7.9854 \cos(2\pi\xi) \cos(2\pi\eta)(\cos^2(2\pi\xi) + \cos^2(2\pi\eta)) \\ & - 25.6631 \cos(2\pi\xi) \cos(2\pi\eta)(\cos(2\pi\xi) + \cos(2\pi\eta)) \\ & - 10.9503(\cos^3(2\pi\xi) + \cos^3(2\pi\eta)) \\ & + 15.0347 \cos(2\pi\xi) \cos(2\pi\eta) + 6.8918(\cos^2(2\pi\xi) + \cos^2(2\pi\eta)) \\ & + 7.4844(\cos(2\pi\xi) + \cos(2\pi\eta)) + 1.4208 = 0. \end{aligned} \tag{100}$$

This can be rewritten as

$$c_d^2 = \frac{c_s^4 - 4.5851 c_s^3 + 3.6089 c_s^2 + 3.7491 c_s + 0.7117}{c_s^2 + 0.9001 c_s + 0.1567} \tag{101}$$

with

$$c_s = \cos(2\pi\xi) + \cos(2\pi\eta), \qquad c_d = \cos(2\pi\xi) - \cos(2\pi\eta). \tag{102}$$

The numerical calculation showed that either c_d^2 from equation (101) is negative or one of the cosines is larger than one. Therefore there is no real solution of this type.

Comparison. The figure for α-cristobalite in [2, 3] shows the RUMs of figures 2 and 4 and the line equation (95) (green) for $\xi, \eta, \zeta \geqslant 0$. The line figure 3 cannot be seen. However, a region of quasi-RUMs (modes of small frequency) is shown, which probably hides the line of figure 3.

3.5. α-quartz

The coordinates of the Si and O ions in α-quartz are

i	$c'_{i,1}$	$c'_{i,2}$	$c'_{i,3}$
1	x_1	0	2/3
2	0	x_1	1/3
3	$-x_1$	$-x_1$	0

i	$c_{i,1}$	$c_{i,2}$	$c_{i,3}$
1	x_2	y_2	z_2
2	$-y_2$	x_2-y_2	$2/3+z_2$
3	y_2-x_2	$-x_2$	$1/3+z_2$
4	y_2	x_2	$-z_2$
5	$-x_2$	y_2-x_2	$2/3-z_2$
6	x_2-y_2	$-y_2$	$1/3-z_2$

$$\mathbf{a}_1 = \tfrac{1}{2}a\mathbf{e}_1 - \tfrac{\sqrt{3}}{2}a\mathbf{e}_2 \qquad \mathbf{a}_2 = \tfrac{1}{2}a\mathbf{e}_1 + \tfrac{\sqrt{3}}{2}a\mathbf{e}_2 \qquad \mathbf{a}_3 = c\mathbf{e}_3. \tag{103}$$

The corners of the three tetrahedra are obtained by applying $\mathcal{A}$ to
the first tetrahedron: $\mathbf{c}_1, \mathbf{c}_2+\mathbf{e}_1-\mathbf{e}_3, \mathbf{c}_5+\mathbf{e}_1+\mathbf{e}_3, \mathbf{c}_6+\mathbf{e}_3$;
the second tetrahedron: $\mathbf{c}_2-\mathbf{e}_3, \mathbf{c}_3+\mathbf{e}_2-\mathbf{e}_3, \mathbf{c}_4+\mathbf{e}_3, \mathbf{c}_6+\mathbf{e}_2+\mathbf{e}_3$; and
the third tetrahedron: $\mathbf{c}_1-\mathbf{e}_3, \mathbf{c}_3+\mathbf{e}_1+\mathbf{e}_2-\mathbf{e}_3, \mathbf{c}_4+\mathbf{e}_3, \mathbf{c}_5+\mathbf{e}_1+\mathbf{e}_2$.
The determinant evaluates to

$$\tilde{\mathcal{M}} = k_1^3(\mathcal{R}_1+\mathcal{R}_2), \tag{104}$$

$$k_1 = \frac{2(3x_2-2)(-2x_2+3z_2x_2-6y_2z_2+5y_2)}{9}, \tag{105}$$

$$\mathcal{R}_1 = f_2(\rho_1,\rho_2)\frac{1-\rho_3^2}{\rho_3}\left(k_2 f_1(\rho_1,\rho_2)+k_3\frac{1+\rho_3^2}{\rho_3}+k_4\right) \tag{106}$$

$$\begin{aligned}\mathcal{R}_2 = {}& \frac{1-\rho_3^4}{\rho_3^2}(k_5 f_1(\rho_1,\rho_2)+k_6)\\ &+\frac{1-\rho_3^2}{\rho_3}(k_7 f_1(\rho_1,\rho_2)+k_8 f_1(\rho_1^2,\rho_2^2)+k_9 f_4(\rho_1,\rho_2)+k_{10})\\ &+\left(k_{11}\frac{1+\rho_3^2}{\rho_3}+k_{12}\right)f_3(\rho_1,\rho_2),\end{aligned} \tag{107}$$

$$f_4(\rho_1,\rho_2) = \frac{(\rho_1+\rho_2)(1+\rho_1\rho_2^2)(1+\rho_1^2\rho_2)}{\rho_1^2\rho_2^2}, \tag{108}$$

with lengthy polynomial expressions of x_2, y_2, z_2 for the constants k_2–k_{12}. With

$$x_2 = 0.4141, \qquad y_2 = 0.2681, \qquad z_2 = 0.7854 \tag{109}$$

from [12] one obtains

$$\begin{aligned} &k_1 = -0.037\,819, && k_2 = 0.018\,997, && k_3 = -0.030\,172,\\ &k_4 = 0.000\,088, && k_5 = 0.006\,248, && k_6 = -0.060\,332,\\ &k_7 = 0.021\,768, && k_8 = -0.009\,082, && k_9 = -0.000\,285,\\ &k_{10} = -0.078\,514, && k_{11} = -0.006\,089, && k_{12} = 0.001\,074. \end{aligned} \tag{110}$$

From the zeros of $\mathcal{R}_1$ combined with the zeros of $\mathcal{R}_2$ one obtains three classes of solutions.
(i) $f_2(\rho_1,\rho_2)=0$ yields a class of RUMs

$$[\xi,0,\zeta(\xi)], \qquad [0,-\xi,\zeta(\xi)], \qquad [-\xi,\xi,\zeta(\xi)] \tag{111}$$

where $\zeta(\xi)$ is determined by

$$\mathcal{R}_2(\rho_1 = \mathrm{e}^{2\pi\mathrm{i}\xi}, \rho_2 = 1, \rho_3 = \mathrm{e}^{2\pi\mathrm{i}\zeta(\xi)}) = 0. \tag{112}$$

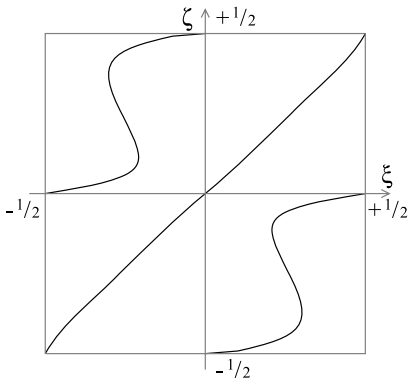

Figure 5. $\zeta(\xi)$ of the RUMs of α-quartz described by equations (111) and (112).

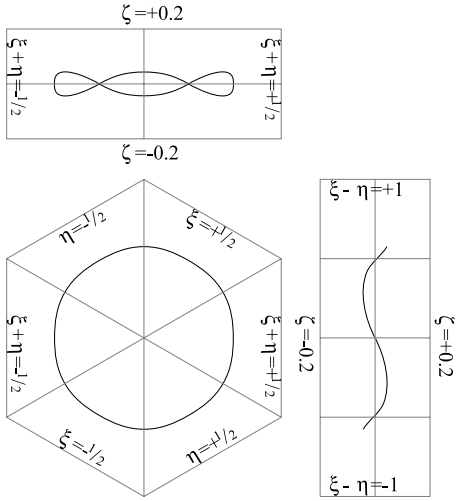

Figure 6. The RUMs given by equation (115) shown in the (ξ, η)-plane and ζ versus $\xi + \eta$ and $\xi - \eta$, respectively, for α-quartz.

The solutions are shown in figure 5. One line of RUMs is nearly straight; the other one is snaky.

(ii) $1 - \rho_3^2 = 0$ and $f_3(\rho_1, \rho_2) = 0$ yield straight lines of RUMs

$$[\xi, \xi, 0], \qquad [\xi, -2\xi, 0], \qquad [-2\xi, \xi, 0], \tag{113}$$

$$[\xi, \xi, 1/2], \qquad [\xi, -2\xi, 1/2], \qquad [-2\xi, \xi, 1/2]. \tag{114}$$

(iii) The condition

$$k_2 f_1(\rho_1, \rho_2) + k_3(\rho_3 + 1/\rho_3) + k_4 = 0, \qquad \mathcal{R}_2 = 0 \tag{115}$$

yields the curve depicted in figure 6. This curve is not a planar curve. The projection onto the $\xi\eta$-plane is nearly a circle. In the ζ-direction it oscillates between -0.0433 and $+0.0433$. Thus it stays close to the $\zeta = 0$ plane. It can be approximately described as a function of the parameter χ:

$$\xi = r(\chi)\sin\left(\frac{\pi}{6} - \chi\right), \qquad \eta = r(\chi)\sin\left(\frac{\pi}{6} + \chi\right),$$
$$r(\chi) = 0.3290 - 0.0035\cos(6\chi), \qquad \zeta = 0.0452\sin(3\chi) + 0.0019\sin(9\chi). \tag{116}$$

This curve intersects with the lines of RUMs (113) at $\chi = k\pi/3$, and with the RUMs given by the curves (111) at $\chi = \pi/6 + k\pi/3$ for integer k.

Comparison. Comparing the distribution of the RUM vectors for α-quartz given in [2, 3] with the curves calculated here, we find agreement for the straight lines and the curves of figure 5. We do not find the non-planar curve of figure 6, equation (116). Since figure 10 of [3] shows only RUMs for positive ζ, this line should run through the dark regions of quasi-RUMs in the figure.

References

[1] Hammonds K D, Dove M T, Giddy A P, Heine V and Winkler B 1996 Rigid-unit phonon modes and structural phase transitions in framework silicates *Am. Mineral.* **81** 1057

[2] CRUSH: The rigid unit mode program http://www.esc.cam.ac.uk/rums/

[3] Dove M T, Pryde A K A, Heine V and Hammonds K D 2007 Exotic distributions of rigid unit modes in the reciprocal space of framework aluminosilicates *J. Phys.: Condens. Matter* **19** 275209

[4] Grimm H and Dorner B 1975 Mechanism of α–β phase transformation of quartz *J. Phys. Chem. Solids* **36** 407

[5] Sartbaeva A, Wells S A, Treacy M M J and Thorpe M F 2006 The flexibility window in zeolites *Nat. Mater.* **5** 962

[6] Goodwin A L, Wells S A and Dove M T 2006 Cation substitution and strain screening: the role of rigid unit modes *Chem. Geol.* **225** 213

[7] Giddy A P, Dove M T, Pawley G S and Heine V 1993 The determination of rigid unit modes as potential soft modes for displacive phase transitions in framework crystal structures *Acta Crystallogr.* A **49** 697

[8] Hammonds K D, Dove M T, Giddy A P and Heine V 1994 CRUSH: a FORTRAN program for the analysis of the rigid unit mode spectrum of a framework structure *Am. Mineral.* **79** 1207

[9] Vallade M, Berge B and Dolino G 1992 Origin of the incommensurate phase of quartz: II. Interpretation of inelastic neutron scattering data *J. Physique* I **2** 1481

[10] Megaw H D 1971 Crystal structures and thermal expansion *Mater. Res. Bull.* **6** 1007

[11] Dove M T, Hammonds K D, Heine V, Withers R L, Xiao Y and Kirkpatrick R J 1996 Rigid unit modes in the high-temperature phase of SiO_2 tridymite: calculations and electron-diffraction *Phys. Chem. Minerals* **23** 56

[12] http://cst-www.nrl.navy.mil/lattice/struk/sio2.html

[13] Wells S, Dove M and Tucker M 2004 Reverse Monte Carlo with geometric analysis—RMC + GA *J. Appl. Crystallogr.* **37** 536